Research article

Rapports De Pharmacie Vol.5 (2), 2019, 556-568
ISSN: 2455-0507

DEVELOPMENT AND OPTIMIZATION OF MONTELUKAST β-CYCLODEXTRIN LOADED LIPOSOMAL GEL

Tan Chin Teng* and Jaya Raja Kumar

**Research student, Asian Institute of Medicine, Science and Technology (AIMST) University, Bedong, 08100, Kedah, Malaysia*

ABSTRACT

This study aims to prepare and optimize Montelukast β-Cyclodextrin loaded liposomal gel. The effect of major independent variables (Cholesterol, Poloxamer 188, and Span 80) on globule size, refractive index, % CDR, viscosity, gel strength and spreadability were studied using Box-Behnken design. Montelukast β-Cyclodextrin loaded liposomal gels were prepared. Various parameters were characterized include, globule size, refractive index, % CDR, viscosity, gel strength and spreadability. Data were analyzed using Stat-Ease Design Expert Software (DX11) to obtain analysis of variance (ANOVA), regression coefficients and regression equation. Optical microscopy was employed to study morphology of the formulations. FTIR and HPLC studies were also performed.

Keywords: Montelukast, β-Cyclodextrin, Liposomes, Liposomal Gel, Box-Behnken Design

INTRODUCTION

Liposomes are microscopic, spherical vesicles made up of phospholipid bilayers enclosing one or more aqueous compartments. Liposomes are widely used in drug delivery system as effective carriers for hydrophilic and lipophilic drugs. [1] β-Cyclodextrins (CDs) are cyclic oligosaccharides, consisting of seven D-(+)-glucopyranose units, which form host-guest inclusion complexes with lipophilic molecules. [2] The ability of CD to increase aqueous solubility of drug used to increase drug entrapment in aqueous compartment of liposomes and liposomes able to protect CD/drug inclusion complexes until drug release, as well as provide sustained drug release mechanism. [3, 4] Thus, the coupling of both delivery systems by encapsulating CD/drug inclusion complex into liposomes is proposed to improve bioavailability and therapeutic efficacy of drug. Liposome gel formulations perform better therapeutic effects than conventional formulations, as it provides prolonged and sustained release dosage forms, leading to improved efficiency and better patient compliance.

Montelukast is a selective leukotriene receptor antagonist used for chronic maintenance treatment of asthma and relief of symptoms of allergic rhinitis by inhibiting leukotriene-induced bronchoconstriction and decreases airway inflammation. [5] In this studies, Montelukast β-cyclodextrin loaded liposomal gel were experimentally prepared with the aim of enhancing bioavalibility and stability of Montelukast due to its poor aqueous solubility, [5] and characterized using factorial design.

Address for correspondence:
Tan Chin Teng,
Research student in pharmacy,
AIMST University,
Bedong- Semeling, Kedah,
Malaysia 08100

MATERIALS

Montelukast purchased from SM Pharmaceuticals Sdn. Bhd., cholesterol and karaya gum procured from Sigma Aldrich Co., β-Cyclodextrin purchased from HiMedia Laboratories Pvt. Ltd., diethyl ether, poloxamer 188, Span 80, HPMC, and xanthan gum procured from Merck Co.

METHOD OF PREPARATION

Formulation of montelukast β-cyclodextrin loaded liposomal gel as shown in figure 1.

IN-VITRO EVALUATION TEST

Globule Size:

Globule size of Montelukast β-Cyclodextrin loaded liposomal gel was determined by using Malvern particle size analyzer (Zetasizer 4000S, Japan).

Refractive index:

Refractive index of the formulations was determined using Abbe refractometer. 1 drop of the formulation was transferred to sample prism and covered. The scale needle was adjusted until a half dark-half bright zone was obtained. The readings were noted by counting the scale number.

Drug Diffusion Studies:

Franz diffusion cell method was applied using phosphate buffer (pH 7.4) at body temperature for in-vitro drug release studies. A cellophane membrane was soaked overnight in phosphate buffer at room temperature. The membrane was then placed between donor and receptor compartment of diffusion cell with an exposed membrane surface area of 2.97 cm^2 to the receptor compartment. The receptor compartment was filled with 16.4 ml of freshly prepared phosphate buffer (pH 7.4) maintained at 37 ± 0.5°C with constant stirring using a Teflon coated magnetic stir bead.

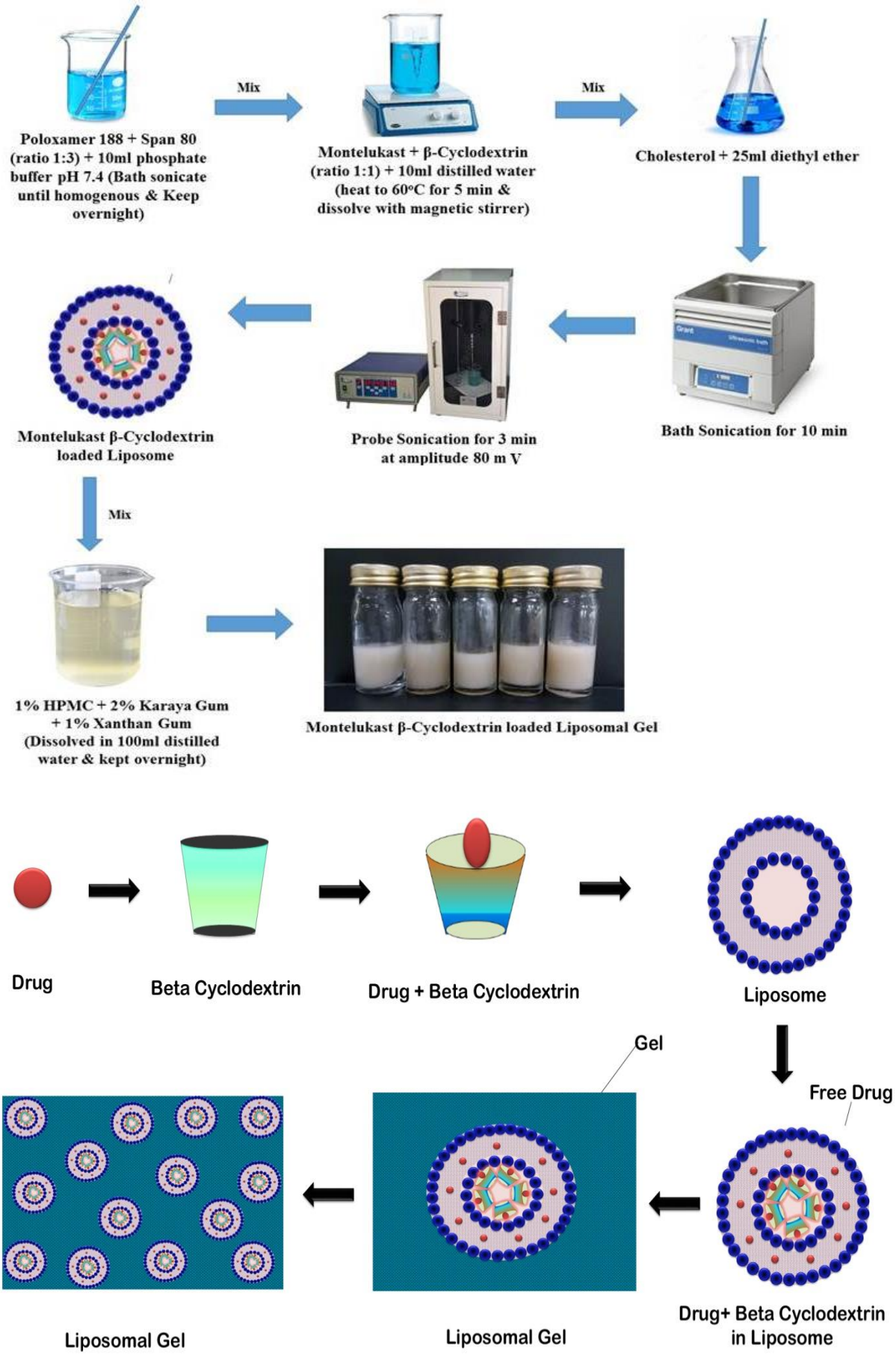

Figure 1: Schematic Diagram of Montelukast β-Cyclodextrin Loaded Liposomal Gel

The liposomal gel equivalent to 1 mg of drug formulation was placed on the membrane and the top of diffusion cell was covered with paraffin paper. At appropriate time intervals, 2 ml aliquots of the receptor medium were withdrawn and immediately replaced with an equal volume of fresh receptor solution to maintain sink conditions. The amount of drug released from liposomal gel was determined by HPLC method. HPLC was carried out at a flow rate of 1.0 ml/min using a mobile phase that is constituted of acetonitrile, 0.5% TEA: ACN (25:75, v/v), and detection was made at 230 nm. A Thermo C18 column (25cm × 4.6mm i.d., 5µ) was used for separation.

Viscosity:

Rheological studies were performed using Brookfield viscometer. Viscosity was determined at 0.3rpm and spindle 63 and the readings were recorded.

Gel Strength

A metal rod with metal discs on both ends and a metal cap through its body was set up. The liposomal gel formulation was filled in a 25ml measuring cylinder. The metal rod was placed in the measuring cylinder and time taken for metal disc to move to the bottom at a distance of 5cm was recorded. The mean readings of three trials were calculated to estimate the gel strength.

Spreadability:

A glass slide was fixed to the table, while another movable glass slide was placed above it and connected to a pan of 72 g weight with the help of cotton thread. Fixed amount of liposomal gel formulations was applied as thin layer between two glass slides and compressed to give uniform thickness. 72 g of weight in the pan was made to float on the air supported by retort stand. Time taken for the movable glass slide to move over the fixed glass slide at a distance of 5 cm was taken. Spreadabiltiy (S) of the formulations was calculated by using equation, $S = \frac{M \times L}{T}$, where S: spreadability (gcm/s), M:weight in the pan (g), L: length moved by the glass slide (cm), and T: time taken to separate the glass slide from each other (s).

pH:

pH of the formulations was determined by using Hanna instruments pH 211 Microprocessor pH meter. Electrodes of pH meter was dipped into formulations and pH values were recorded when it stabilized.

RESULTS & DISCUSSION

Experimental Design of Montelukast β-Cyclodextrin Loaded Liposomal Gel:

In this work, we reported the successful effect on the formulation of Montelukast β-cyclodextrin loaded liposomal gel. Cholesterol (A), Poloxamer 188 (B), and Span 80 (C) were acknowledged as the most significant variables that influence globule size, refractive index, % CDR, viscosity, gel strength, and spreadability. Box-Behnken design (BBD) is used for exploring quadratic response surfaces and constructing second order polynomial models. It consists of simulated center points and the set of points lying at the midpoint of each edge of the multi-dimensional cube.

Based on BBD, twenty runs were essential for response surface methodology. The factor combinations which produced different responses are illustrated in Table 1. These results clearly indicate that all the dependent variables are significantly influenced by selected independent variables. Data were analyzed using Stat-Ease Design-Expert software (DX11) to obtain analysis of variance (ANOVA), regression coefficients and regression equation.

Data normality was proved through normal % probability plot of the externally studentized residuals. The residuals distribute normally if points on the plot lie on a straight line as demonstrated in Figure 2a, b, c, d, e and f.

Graphs of externally studentized residuals vs. predicted values were plotted to test the assumption of constant variance, as illustrated in Figure 3a, b, c, d, e and f. The studentized residuals were located by dividing the residuals by their standard deviations. The points scattered randomly between the outlier detection limits -3.5 to +3.5 and -4.5 to +4.5.

Both residuals vs. predicted and residuals vs. run were scattered randomly. It therefore indicates that the model is suitable for use and can be used to identify the optimal parameters. The residuals vs. run plots for R1 to R6 are quite satisfactory as shown in Figure 4a, b, c, d, e and f. Besides, a high correlation between observed and predicted data indicates their low discrepancies.

The plot of predicted response vs. actual response performs the same function, albeit graphically and also helps to detect the points where the model becomes inadequate to predict response of the system. This graph shows that the selected model is capable of predicting the response satisfactorily within the range of data set as shown in Figure 5a, b, c, d, e and f.

Table 1: Factorial Design of Montelukast β-Cyclodextrin Loaded Liposomal Gel

Run	F1	F2	F3	R1	R2	R3	R4	R5	R 6
	A:Chole-sterol mg	B: Poloxamer 188 mg	C: Span 80 mg	Globule Size µm	Refractive Index	CDR %	Viscosity cps	Gel Strength s	Spread-ability g.cm/s
1	125	2000	2000	2.84	1.337	88.74	6999	1.5	12.77
2	167.04	2000	2000	3.2	1.336	80.65	11198	4.17	22.15
3	125	2000	2000	2.96	1.337	88.61	6989	1.55	12.7
4	150	3000	1000	1.96	1.337	80.23	9898	2.04	19.32
5	100	1000	1000	2.36	1.336	90.14	11797	3.42	33.55
6	100	3000	3000	4	1.337	91.02	16796	6.19	34.58
7	150	3000	3000	3.52	1.336	80.65	16996	5.69	38.63
8	100	1000	3000	1.64	1.335	90.45	16896	8.56	37.31
9	125	3681.79	2000	3.44	1.337	87.99	12297	1.38	26.16
10	125	2000	318.207	2.2	1.337	88.11	8398	1.05	15.44
11	100	3000	1000	1.48	1.337	91.45	9398	1.15	14.45
12	125	2000	2000	2.88	1.337	88.31	6970	1.62	12.73
13	125	2000	3681.7	2.96	1.335	88.01	10897	6.74	25.71
14	125	318.207	2000	2.04	1.334	89.01	13597	4.35	33.32
15	82.95	2000	2000	1.72	1.335	95.18	13497	3.08	43.99
16	150	1000	3000	1.76	1.334	83.45	14997	7.41	47.04
17	125	2000	2000	2.8	1.336	87.99	6975	1.57	12.72
18	150	1000	1000	2.26	1.337	82.66	12097	1.63	22.96
19	125	2000	2000	3.02	1.337	87.34	6999	1.52	12.75
20	125	2000	2000	2.76	1.337	87.85	6999	1.54	12.74

Box-Cox Plot for Power Transforms provides a guideline that help to select the correct power law transformation, based on the best λ value. Transformation parameter, λ is chosen such that it maximized the log-likelihood function. The maximum likelihood estimate of λ agrees to the value for which the squared sum of errors from the fitted model is a minimum. This value of λ is determined by fitting a diverse range of λ values and choosing the value corresponding to the minimum squared sum of errors. t can also be chosen graphically from the Box-Cox normality plot. Value of λ=1.00 indicates that no transformation needed and produces results identical to original data shown in Figure 6a, b, c, d, e and f.

Plot of residuals vs. factor A (Cholesterol), as shown in Figure 7a, b, c, d, e and f, is used to check whether the variance not accounted for by the model is different for various levels of A. The plot exhibits a random scatter if the result is satisfactory. Pronounced curvature may indicate a systematic contribution of the independent factor that is not accounted for by the model.

Cook's distance (Di) is a product of the square of the i^{th} internally studentized residual and a monotonic function of the leverage. The plot is a measure of how much the entire regression function changes when the i^{th} point is not included for fitting the model. It is essentially the sum of differences in predictions at every point caused by leaving a point out for fitting the model. Cook's distance plots for R1 to R6 are shown in Figure 8a, b, c, d, e and f respectively.

Figure 9a, b, c, d, e and f show the plot of leverage vs. run for R1 to R6 respectively. Leverage of a point varies from 0 to 1 and it indicates how much an individual design point influences the model's predicted values. If a point has a leverage of 1.0, predicted value at that particular case exactly equal the observed value of the experiment and such, the residual will be 0. The sum of leverage values across all cases equals the number of coefficients (including the constant) fit by the model. The maximum leverage an experiment can have is 1/k, where k is the number of times the experiment is replicated.

DFFITS is a measure of how much the prediction changes at the i^{th} point when the i^{th} point is not included for fitting the model. It measures the influence the i^{th} observation has on the predicted value. DFFITS versus run plots are shown in Figure 10a, b, c, d, e and f respectively.

DFBETAS is a measure of how much a coefficient estimate changes when the i^{th} point is not used to fit the model. It shows the influence the i^{th} observation has on each regression coefficient. There are separate DFBETAS plots for each term in the model, as depicted in Figure 11a, b, c, d, e and f.

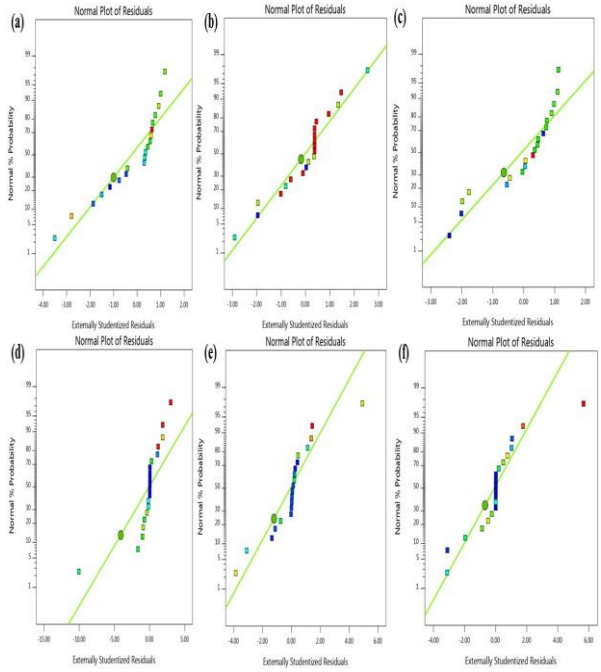

Figure 2: (a) Normal % probability plot of the externally studentized residuals (R1). (b) Normal % probability plot of the externally studentized residuals (R2). (c) Normal % probability plot of the externally studentized residuals (R3). (d) Normal % probability plot of the externally studentized residuals (R4). (e) Normal % probability plot of the externally studentized residuals (R5). (f) Normal % probability plot of the externally studentized residuals (R6).

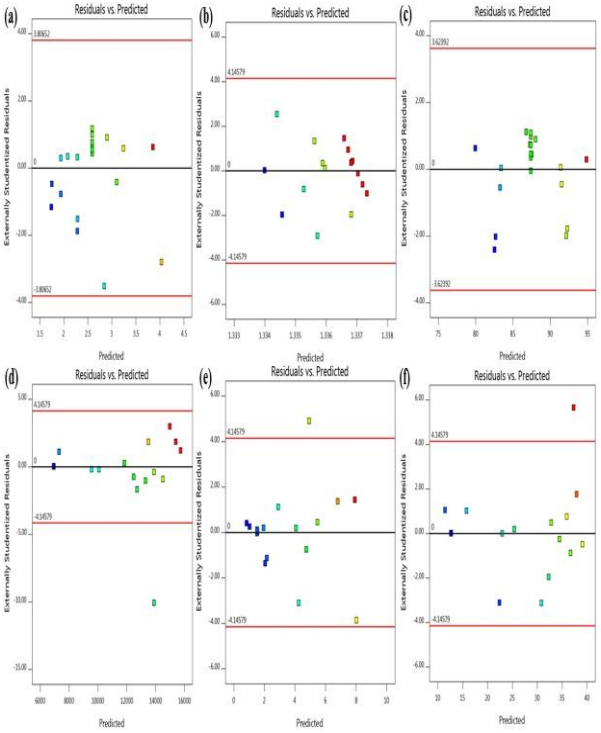

Figure 3: (a) Residuals vs. Predicted (R1). (b) Residuals vs. Predicted (R2). (c) Residuals vs. Predicted (R3). (d) Residuals vs. Predicted (R4). (e) Residuals vs. Predicted (R5). (f) Residuals vs. Predicted (R6).

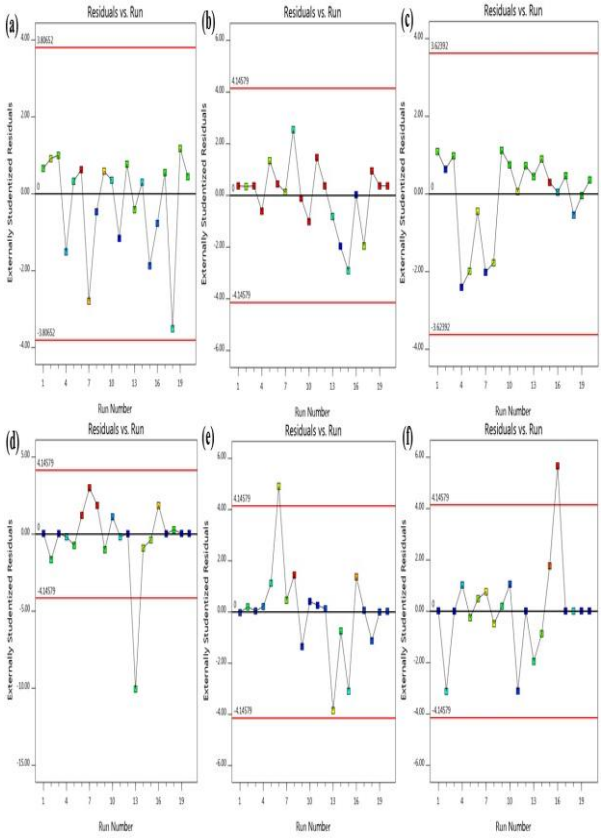

Figure 4: (a) Residuals vs. Run (R1). (b) Residuals vs. Run (R2). (c) Residuals vs. Run (R3). (d) Residuals vs. Run (R4). (e) Residuals vs. Run (R5). (f) Residuals vs. Run (R6).

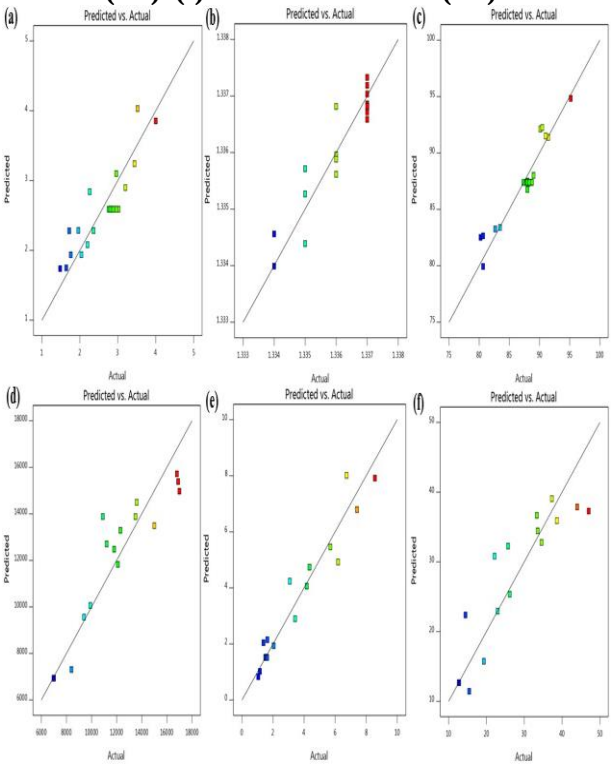

Figure 5: (a) Predicted vs. Actual (R1). (b) Predicted vs. Actual (R2). (c) Predicted vs.

Actual (R3). (d) Predicted vs. Actual (R4). (e) Predicted vs. Actual (R5). (f) Predicted vs. Actual (R6).

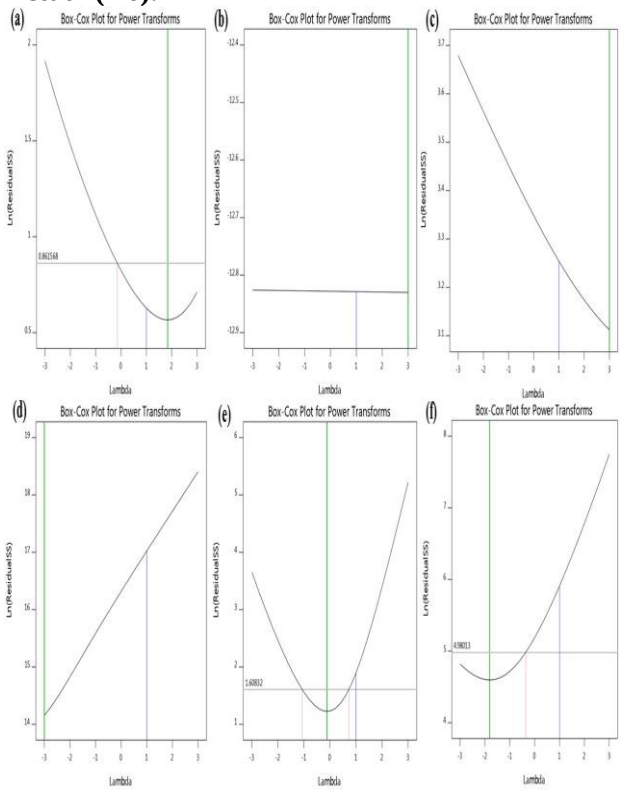

Figure 6: (a) Box-Cox Plot (R1). (b) Box-Cox Plot (R2). (c) Box-Cox Plot (R3). (d) Box-Cox Plot (R4). (e) Box-Cox Plot (R5). (f) Box-Cox Plot (R6).

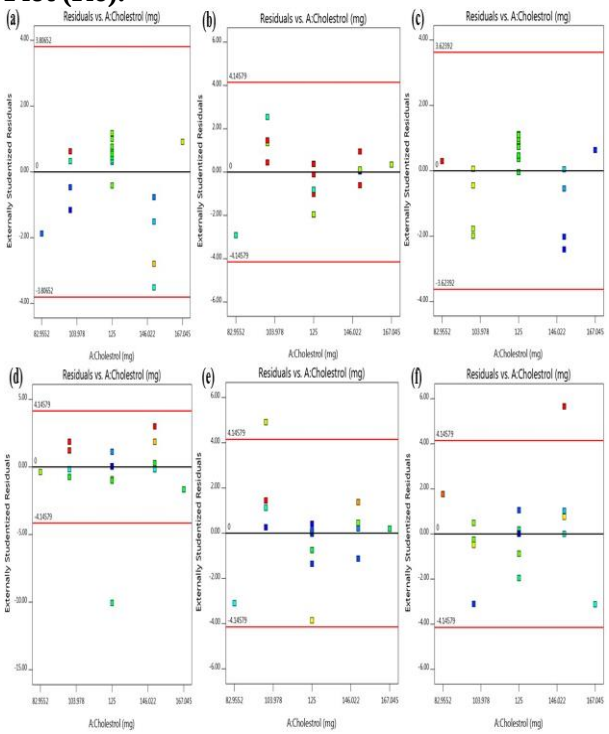

Figure 7: (a) Residuals vs. Factor A Cholesterol (R1). (b) Residuals vs. Factor A Cholesterol (R2). (c) Residuals vs. Factor A Cholesterol (R3). (d) Residuals vs. Factor A Cholesterol (R4). (e) Residuals vs. Factor A Cholesterol (R5). (f) Residuals vs. Factor A Cholesterol (R6)

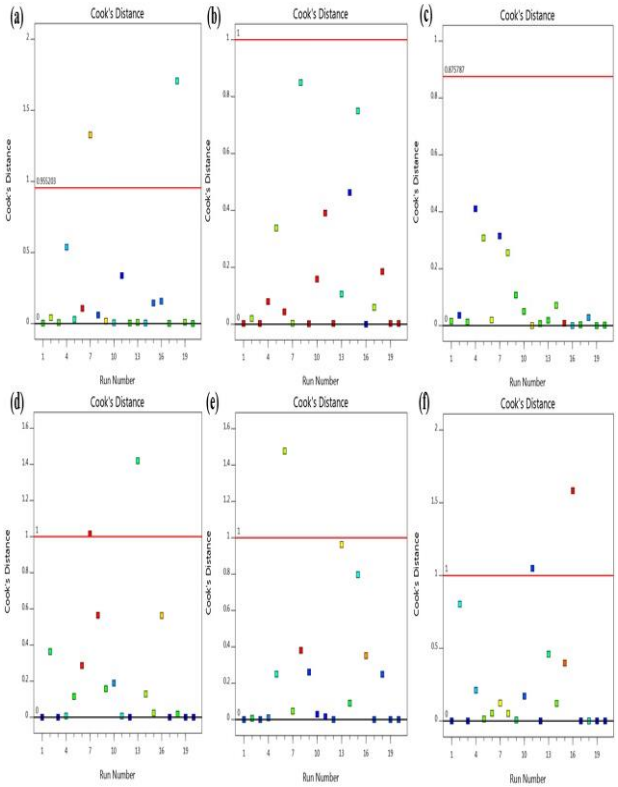

Figure 8: (a) Cook's Distance plot (R1). (b) Cook's Distance plot (R2). (c) Cook's Distance plot (R3). (d) Cook's Distance plot (R4). (e) Cook's Distance plot (R5). (f) Cook's Distance plot (R6).

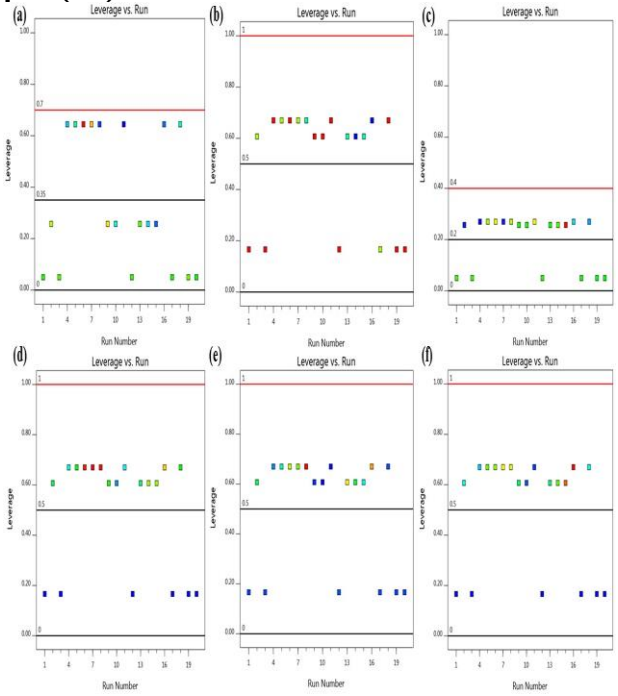

Figure 9: (a) Leverage vs. Run (R1). (b) Leverage vs. Run (R2). (c) Leverage vs. Run (R3). (d) Leverage vs. Run (R4). (e) Leverage vs. Run (R5). (f) Leverage vs. Run (R6).

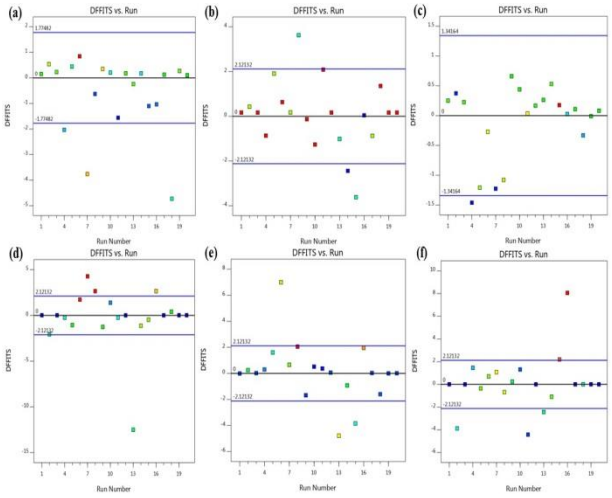

Figure 10: (a) DFFITS vs. Run (R1). (b) DFFITS vs. Run (R2). (c) DFFITS vs. Run (R3). (d) DFFITS vs. Run (R4). (e) DFFITS vs. Run (R5). (f) DFFITS vs. Run (R6).

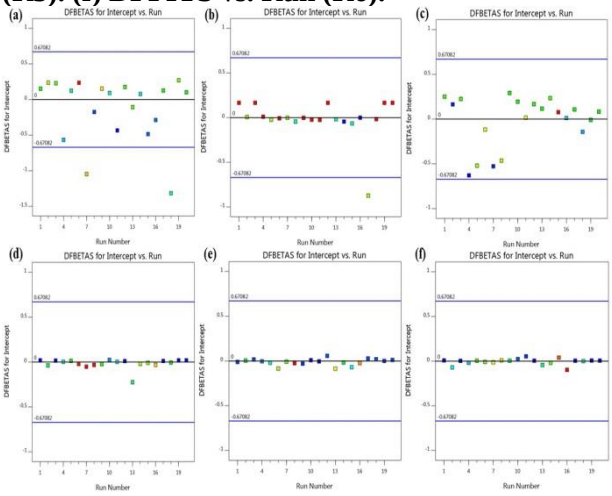

Figure 11: (a) DFBETAS for Intercept vs. Run (R1). (b) DFBETAS for Intercept vs. Run (R2). (c) DFBETAS for Intercept vs. Run (R3). (d) DFBETAS for Intercept vs. Run (R4). (e) DFBETAS for Intercept vs. Run (R5). (f) DFBETAS for Intercept vs. Run (R6).

Montelukast β-cyclodextrin loaded liposomal gel showed globule size between the ranges of 1.48-4 µm as shown in Table 1 and Figure 12. A good correlation coefficient (1.000) is exhibited in factorial equation for globule size and the Model F-value of 8.50 (P-value: 0.0007) which implies that the model is significant. Since P-values < 0.05 indicate the model term are significant, in this case, B, C, and BC are significant model terms as shown in Table 2. The Lack of Fit F-value of 23.59 implies the Lack of Fit is significant. There is only a 0.15% chance that a Lack of Fit F-value this large could occur due to noise. The effects of B and C are more significant than A. The individual main effects of A, B and C on R1 are as shown in Figure 13a. The 2D contour, 3D response surfaces plots and 3D cube plots of R1 are shown in Figure 13b, c, and d to depict the interactive effects of A and B on R1, at constant level of C. The shape of response surfaces and contour plots reveal the nature and extent of interaction between different factors.

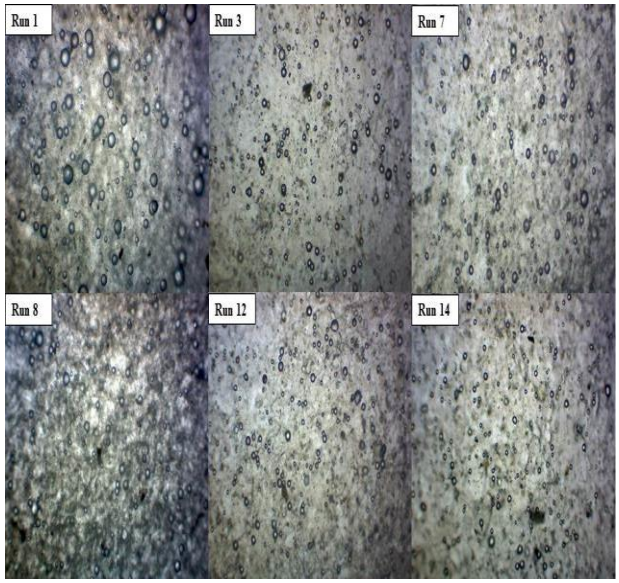

Figure 12: Optical Microscopy of Montelukast β-Cyclodextrin Loaded Liposomal Gel

Table 2: ANOVA results of Quadratic Mod-el for response Globule Size (R1)

Source	Sum of Squares	df	Mean Square	F-value	p-value	
Model	7.35	6	1.22	8.50	0.0007	significant
A-Cholesterol	0.4610	1	0.4610	3.20	0.0969	
B-Poloxamer188	2.05	1	2.05	14.25	0.0023	
C-Span 80	1.25	1	1.25	8.71	0.0113	
AB	0.0000	1	0.0000	0.0003	0.9854	
AC	0.0685	1	0.0685	0.4752	0.5027	
BC	3.51	1	3.51	24.38	0.0003	
Residual	1.87	13	0.1440			
Lack of Fit	1.82	8	0.2280	23.59	0.0015	significant
Pure Error	0.0483	5	0.0097			
Cor Total	9.22	19				

Table 3: ANOVA results of Quadratic Model for response refractive index (R2)

Source	Sum of Squares	df	Mean Square	F-value	p-value	
Model	0.0000	9	2.057	7.67	0.0019	significant
A-Cholesterol	3.404	1	3.404	0.1269	0.7291	
B-Poloxamer188	7.389	1	7.389	27.54	0.0004	
C-Span 80	5.122	1	5.122	19.09	0.0014	
AB	1.250	1	1.250	0.4660	0.5103	
AC	1.125	1	1.125	4.19	0.0677	
BC	1.125	1	1.125	4.19	0.0677	
A^2	1.865	1	1.865	6.95	0.0249	
B^2	1.865	1	1.865	6.95	0.0249	
C^2	4.825	1	4.825	1.80	0.2095	
Residual	2.683	10	2.683			
Lack of Fit	1.849	5	3.698	2.22	0.2011	not significant
Pure Error	8.333	5	1.667			
Cor Total	0.0000	19				

Table 4: ANOVA results of Quadratic Model for response % CDR (R3)

Source	Sum of Squares	df	Mean Square	F-value	p-value	
Model	270.01	3	90.00	55.62	< 0.0001	significant
A-Cholesterol	268.07	1	268.07	165.65	< 0.0001	
B-Poloxamer188	1.88	1	1.88	1.16	0.2972	
C-Span 80	0.0622	1	0.0622	0.0384	0.8470	
Residual	25.89	16	1.62			
Lack of Fit	24.54	11	2.23	8.22	0.0153	significant
Pure Error	1.36	5	0.2713			
Cor Total	295.91	19				

Table 5: ANOVA results of Quadratic Model for response viscosity (R4)

Source	Sum of Squares	df	Mean Square	F-value	p-value	
Model	2.192	9	2.435	9.85	0.0007	significant
A-Cholesterol	1.663	1	1.663	0.6723	0.4313	
B-Poloxamer188	1.748	1	1.748	0.7066	0.4202	
C-Span 80	5.219	1	5.219	21.10	0.0010	
AB	6.607	1	6.607	0.2671	0.6165	
AC	7.806	1	7.806	0.3156	0.5866	
BC	5.276	1	5.276	2.13	0.1748	
A^2	7.290	1	7.290	29.47	0.0003	
B^2	8.729	1	8.729	35.29	0.0001	
C^2	2.415	1	2.415	9.76	0.0108	
Residual	2.473	10	2.473			
Lack of Fit	2.473	5	4.946	28908.99	< 0.0001	significant
Pure Error	855.50	5	171.10			
Cor Total	2.439	19				

Table 6: ANOVA results of Quadratic Model for response Gel Strength (R5)

Source	Sum of Squares	df	Mean Square	F-value	p-value	
Model	101.86	9	11.32	17.01	< 0.0001	significant
A-Cholesterol	0.0376	1	0.0376	0.0566	0.8168	
B-Poloxamer188	8.77	1	8.77	13.18	0.0046	
C-Span 80	62.35	1	62.35	93.71	< 0.0001	
AB	1.39	1	1.39	2.08	0.1795	
AC	0.0703	1	0.0703	0.1057	0.7518	
BC	0.6216	1	0.6216	0.9343	0.3565	
A^2	12.48	1	12.48	18.76	0.0015	
B^2	6.31	1	6.31	9.49	0.0116	
C^2	15.17	1	15.17	22.81	0.0008	
Residual	6.65	10	0.6653			
Lack of Fit	6.64	5	1.33	755.05	< 0.0001	significant
Pure Error	0.0088	5	0.0018			
Cor Total	108.51	19				

Table 7: ANOVA results of Quadratic Model for response spreadability (R6)

Source	Sum of Squares	df	Mean Square	F-value	p-value	
Model	2196.89	9	244.10	6.62	0.0034	significant
A-Cholesterol	60.19	1	60.19	1.63	0.2301	
B-Poloxamer188	154.41	1	154.41	4.19	0.0679	
C-Span 80	523.48	1	523.48	14.20	0.0037	
AB	11.96	1	11.96	0.3244	0.5815	
AC	47.53	1	47.53	1.29	0.2826	
BC	16.82	1	16.82	0.4564	0.5146	
A^2	847.54	1	847.54	23.00	0.0007	
B^2	607.29	1	607.29	16.48	0.0023	
C^2	152.33	1	152.33	4.13	0.0695	
Residual	368.55	10	36.86			
Lack of Fit	368.55	5	73.71	1.249	< 0.0001	significant
Pure Error	0.0029	5	0.0006			
Cor Total	2565.44	19				

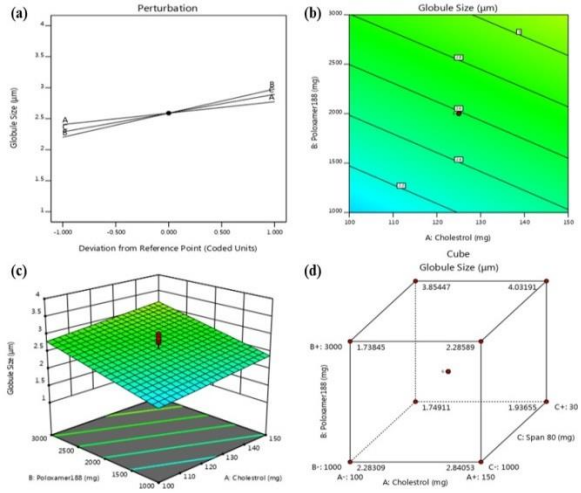

Figure 13: (a) Perturbation plot showing the individual effect of Cholesterol (A), Poloxamer 188 (B), and Span 80 (C) on globule size (R1). (b) 2D response surface plot presenting the interaction between A and B affecting R1 at constant C. (c) 3D response surface plot presenting the interaction between A and B affecting R1 at constant C. (d) 3D cube plot of Box-Behnken design (R1).

The mathematical model generated for refractive index (R2) was found to be significant with F value of 7.67 (p-value: 0.0019) and R^2 value of 0.8735. Model terms of B, C, A^2 and B^2 have significant effects on R2, since P-values <0.05 represent the significant model terms as shown in Table 3. The Lack of Fit F-value of 2.22 implies the Lack of Fit is not significant relative to the pure error. There is a 20.11% chance that a Lack

of Fit F-value could occur. Perturbation plot showing the individual effects of A, B and C on R2 are shown in Figure 14a. The relationship between A and B on R2 at constant C was further elucidated using 2D contour plots, 3D response surfaces plot and 3D cube plot as shown in Figure 14b, c and d.

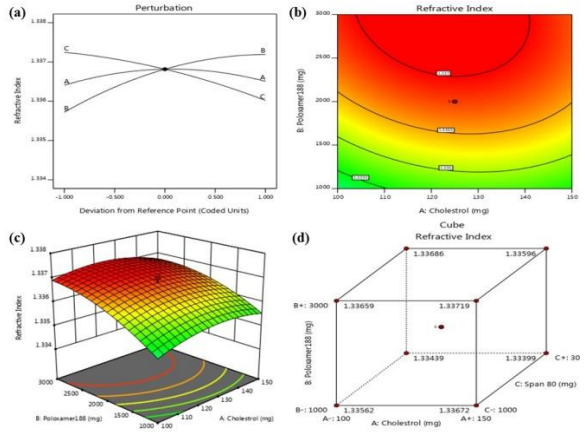

Figure 14: (a) Perturbation plot showing the indivdual effect of Cholesterol (A), Poloxamer 188 (B), and Span 80 (C) on refractive index (R2). (b) 2D response surface plot presenting the interaction between A and B affecting R2 at constant C. (c) 3D response surface plot presenting the interaction between A and B affecting R2 at constant C. (d) 3D cube plot of Box-Behnken design (R2).

The precise model produced for % CDR (R3) was found to be significant with F value of 55.62 (p <0.0001) and R^2 value of 0.9125. A is a significant model term on the % CDR (R3), since the P value < 0.05 indicate model terms are significant as shown in Table 4. The Lack of Fit F-value of 8.22 implies the Lack of Fit is significant. There is only a 1.53% chance that a Lack of Fit F-value could occur due to noise. Perturbation plot showing the main effects of A, B and C on % CDR (R3) are shown in Figure 15a. The correlation between independent variables on R3 was further elucidated using 2D contour plots, 3D response surfaces plot and 3D cube plot as shown in Figure 15b, c and d.

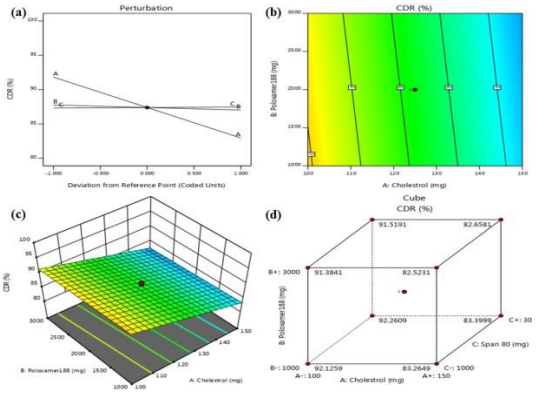

Figure 15: (a) Perturbation plot showing the individual effect of Cholesterol (A), Poloxamer 188 (B), and Span 80 (C) on % CDR (R3). (b) 2D response surface plot presenting the interaction between A and B affecting R3 at constant C. (c) 3D response surface plot presenting the interaction between A and B affecting R3 at constant C. (d) 3D cube plot of Box-Behnken design (R3).

The mathematical model generated for viscosity (R4) was found to be significant with F value of 9.85 (p: 0.0007) and R^2 value of 0.8986. C, A^2, B^2, and C^2 represent the significant model on R4 as shown in Table 5. The Lack of Fit F-value of 28908.99 implies the Lack of Fit is significant. There is only a 0.01% chance that a Lack of Fit F-value could occur. The perturbation plot showing the main effects of A, B and C on R4 are shown in Figure 16a. The correlation between independent variables on R4 was elucidated using 2D contour plots, 3D response surfaces plot and 3D cube plot as shown in Figure 16b, c and d.

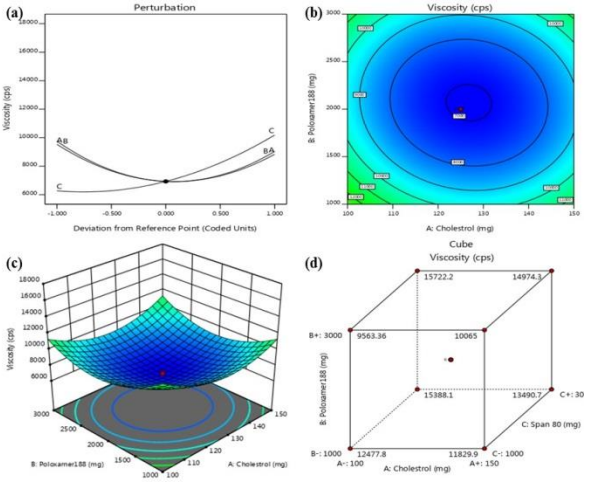

Figure 16: (a) Perturbation plot showing the individual effect of Cholesterol (A), Poloxamer 188 (B), and Span 80 (C) on viscosity (R4). (b) 2D response surface plot presenting the interaction between A and B affecting R4 at constant C. (c) 3D response surface plot presenting the interaction between A and B affecting R4 at constant C. (d) 3D cube plot of Box-Behnken design (R4).

The mathematical model produced for gel strength (R5) was found to be significant with F value of 17.01 (p < 0.0001) and R^2 value of 0.9387. B, C, A^2, B^2, and C^2 represent the significant model terms on R5 as shown in Table 6. The Lack of Fit F-value of 755.05 implies the Lack of Fit is significant. There is only a 0.01% chance that a Lack of Fit F-value this large could occur due to noise. Perturbation plot showing the main effects of A, B and C on R5 are shown in Figure 17a. The

correlation between independent variables on R5 was elucidated using 2D contour plots, 3D response surfaces plot and 3D cube plot as shown in Figure 17b, c and d.

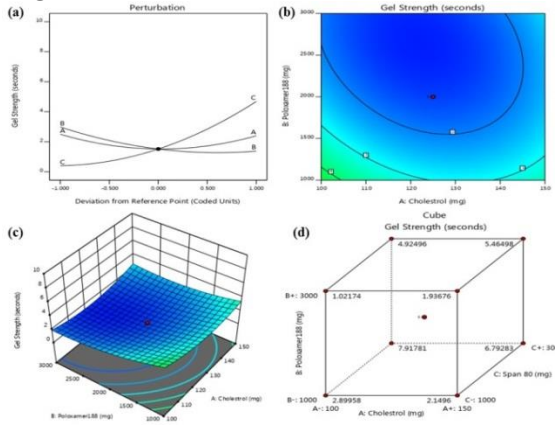

Figure 17: (a) Perturbation plot showing the individual effect of Cholesterol (A), Poloxamer 188 (B), and Span 80 (C) on gel strength (R5). (b) 2D response surface plot presenting the interaction between A and B affecting R5 at constant C. (c) 3D response surface plot presenting the interaction between A and B affecting R5 at constant C. (d) 3D cube plot of Box-Behnken design (R5).

The model of spreadability (R6) showed F value of 6.62 (p-value: 0.0034) and R^2 value of 0.8563 which indicated that the model is significant. Since the P value < 0.05 indicate model terms are significant as shown in Table 7, C, A^2, and B^2 represent the significant model terms on R6. The Lack of Fit F-value of 124932.65 implies the Lack of Fit is significant. There is only 0.01% of chance that a Lack of Fit F-value could occur due to noise. The perturbation plot showing the main effects of A, B and C on R6 are shown in Figure 18a. The correlation between independent variables on R6 was further elucidated using 2D contour plots, 3D response surfaces plot and 3D cube plot as shown in Figure 18b, c and d. Figure 18c shows the interactive effect between A and B on spreadability at constant C.

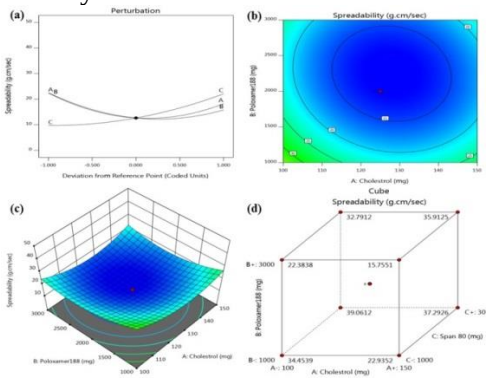

Figure 18: (a) Perturbation plot showing the individual effect of Cholesterol (A), Poloxamer 188 (B), and Span 80 (C) on spreadability (R6). (b) 2D response surface plot presenting the interaction between A and B affecting R6 at constant C. (c) 3D response surface plot presenting the interaction between A and B affecting R6 at constant C. (d) 3D cube plot of Box-Behnken design (R6).

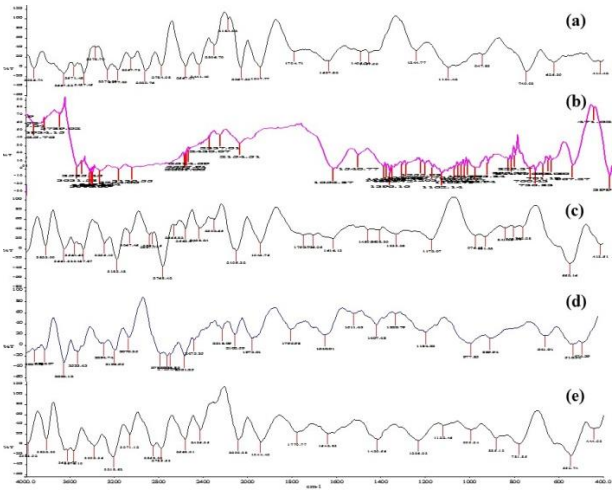

Figure 19: (a) FTIR spectrum of Montelukast. (b) FTIR spectrum of β-Cyclodextrin. (c) FTIR spectrum of Cholesterol. (d) FTIR spectrum of Poloxamer 188. (e) FTIR spectrum of mixture of Montelukast, β-Cyclodextrin, Cholesterol and Poloxamer 188.

Figure 19a showed FTIR spectrum of Montelukast with principal peaks at wavenumbers (cm^{-1}) of 3936.74, 3667.32, 3571.48, 3487.85, 3378.79, 3270.09, 3197.29, 3057.73, 2929.76, 2784.98, 2567.01, 2441.49, 2306.70, 2184.92, 2067.30, 1947.77, 1794.71, 1637.80, 1495.74, 1457.99, 1244.77, 1101.42, 947.83, 749.93, 625.39, and 414.42.

Figure 19b showed FTIR spectrum of β-cyclodextrin with principal peaks at wavenumbers (cm^{-1}) of 3934.15, 3789.02, 3631.53, 3585.45, 3581.09, 3423.44, 3421.44, 3254.66, 3136.55, 2661.00, 2648.25, 2637.91, 2614.69, 2430.07, 2337.01, 2154.51, 1652.87, 1540.77, 1421.60, 1414.16, 1396.16, 1382.72, 1255.98, 1203.02, 1162.14, 1103.79, 1070.42, 1058.17, 1043.51, 1031.84, 856.20, 844.15, 829.37, 760.43, 736.83, 701.19, 678.07, 668.86, 567.27, 471.62.

Figure 19c showed FTIR spectrum of Cholesterol with principal peaks at wavenumbers (cm^{-1}) of 3823.99, 3661.33, 3564.63, 3487.87, 3295.19, 3183.18, 3067.46, 2887.71, 2861.15, 2768.42, 2665.82, 2563.07, 2438.24, 2302.65, 2105.32, 1943.75, 1750.70, 1706.05, 1616.13, 1459.89, 1408.30, 1333.08, 1172.07, 976.13, 931.23, 841.19, 802.76, 782.28, 552.16 and 413.51.

Figure 19d showed FTIR spectrum of Poloxamer 188 with principal peaks at wavenumbers (cm^{-1}) of 3927.83, 3836.07, 3662.12, 3533.43, 3294.74, 3198.95, 3070.35, 2783.37, 2723.04, 2688.85, 2561.25, 2475.35, 2218.09, 2102.59, 1973.01, 1795.98, 1640.01, 1511.43, 1407.48, 1320.79, 1184.23, 977.85, 889.94, 641.01, 516.34 and 474.39.

Figure 19e shows FTIR spectrum of mixture of Montelukast, β-Cyclodextrin, Cholesterol and Poloxamer 188 with principal peaks at wavenumbers (cm^{-1}) of 3988.92, 3822.30, 3631.77, 3576.10, 3392.36, 3218.52, 3071.12, 2858.38, 2785.53, 2568.01, 2436.35, 2090.38, 1944.40, 1779.77, 1642.83, 1420.56, 1236.03, 1122.46, 999.34, 885.13, 781.85, 550.74 and 444.03.

Evaluation of Optimized Montelukast β-Cyclodextrin loaded Liposomal Gel:

Three batches of Montelukast β-Cyclodextrin loaded liposomal gel (Run 2, Run 5 and Run 13) were prepared according to the optimized levels after the polynomial equations relating independent and dependent variables were constructed. The conditions of optimization were acquired by setting constraints on both of the independent and dependent variables. The observed values were in close agreement with the predicted values of the optimized process as shown in Table 8 and 9, thereby demonstrating the feasibility.

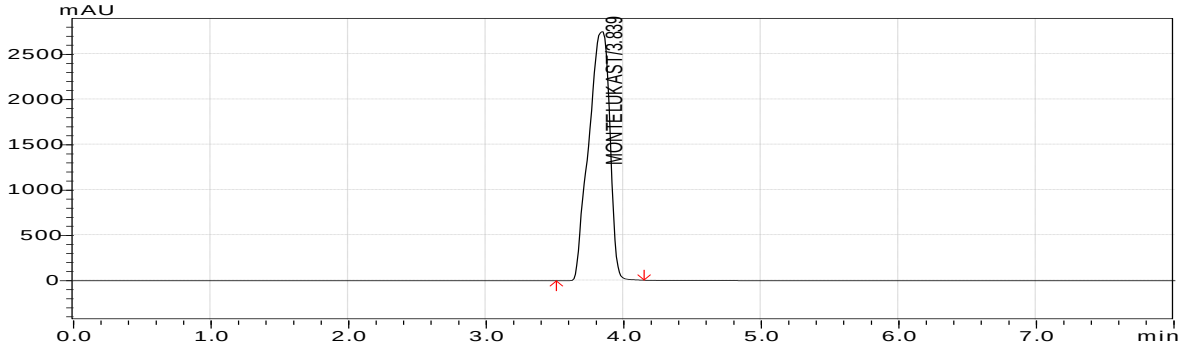

Figure 20: HPLC chromatogram of Montelukast

Table 8: Predicted Values

Independent Variable	Values	Predicted Values					
		Globule Size, R1 (µm)	Refractive Index, R2	% CDR, R3	Viscosity, R4 (cps)	Gel Strength, R5 (s)	Spreadability, R6 (g.cm/s)
Cholesterol (A)	125	2.57098	1.33528	83.252	10865.5	4.7804	27.5796
Poloxamer 188 (B)	2000						
Span 80 (C)	2000						

Table 9: Observed Values

Code	Observed Values					
	Globule Size, R1 (µm)	Refractive Index, R2	% CDR, R3	Viscosity, R4 (cps)	Gel Strength, R5 (s)	Spreadability, R6 (g.cm/s)
R2	3.20	1.336	80.65	11198	4.17	22.15
R5	2.36	1.336	90.14	11797	3.42	33.44
R13	2.96	1.335	88.01	10897	5.74	25.71

CONCLUSION

In this study, Montelukast β-Cyclodextrin loaded liposomal gels were successfully prepared. Various parameters were characterized include, globule size, refractive index, % CDR, viscosity, gel strength and spreadability. Optimization was done based on the results obtained from the formulations coincide with the expected values of various parameters by using Stat-Ease DesignExpert software (DX11). The optimal formulation has a globule size of 2.571µm, refractive index of 1.335, CDR of 83.25%, viscosity of 10865.5 cps, gel strength of 4.780 s,

and spreadability of 27.58 g.cm/s. Optical microscopy images showed uniform, spherical-shaped globules. On the other hand, FTIR results showed that the components used in formulations are compatible. HPLC chromatogram depicted a sharp peak of Montelukast at 3.839 minutes.

REFERENCES

[1] A Akbarzadeh, R Rezaei-Sadabady, S Davaran, S Joo, N Zarghami, Y Hanifehpour et al. Liposome: Classification, Preparation, and Applications. *Nanoscale Research Letters*. 8(1):102 (2013).

[2] D Duchêne, D Wouessidjewe, G Ponchel. Cyclodextrins and Carrier Systems. *Journal of Controlled Release*. 62(1-2):263-268 (1999).

[3] L Fraceto, R Grillo, E Sobarzo-Sanchez. Cyclodextrin Inclusion Complexes Loaded in Particles as Drug Carrier Systems. *Current Topics in Medicinal Chemistry*. 14(4):518-525 (2014).

[4] R Gharib, H Greige-Gerges, S Fourmentin, C Charcosset, L Auezova. Liposomes Incorporating Cyclodextrin–Drug Inclusion Complexes: Current State of Knowledge. *Carbohydrate Polymers*. 129:175-186 (2015).

[5] J Barbosa, F Almeida Paz, S Braga. Montelukast Medicines of Today and Tomorrow: From Molecular Pharmaceutics to Technological Formulations. *Drug Delivery*. 23(9):3257-3265 (2016).

[6] A Laouini, C Jaafar-Maalej, I Limayem-Blouza, S Sfar, C Charcosset, Fessi H. Preparation, Characterization and Applications of Liposomes: State of the Art. *Journal of Colloid Science and Biotechnology*. 1(2):147-168 (2012).

[7] J Chen, W Lu, W Gu, S Lu, Z Chen, B Cai et al. Drug-in-Cyclodextrin-in-Liposomes: A Promising Delivery System for Hydrophobic Drugs. *Expert Opinion on Drug Delivery*. 11(4): 565-577 (2014).

[8] B McCormack, G Gregoriadis. Entrapment of Cyclodextrin-Drug Complexes into Liposomes: Potential Advantages in Drug Delivery. *Journal of Drug Targeting*. 2(5):449-454 (1994).

[9] S Carneiro, F Costa Duarte, L Heimfarth, J Siqueira Quintans, L Quintans-Júnior, V Veiga Júnior et al. Cyclodextrin–Drug Inclusion Complexes: In Vivo and In Vitro Approaches. *International Journal of Molecular Sciences*. 20(3):642 (2019).

[10] A Samad, Y Sultana, M Aqil. Liposomal Drug Delivery Systems: An Update Review. *Current Drug Delivery*. 4(4):297-305 (2007).

[11] J Zhang, P Ma. Cyclodextrin-Based Supramolecular Systems for Drug Delivery: Recent Progress and Future Perspective. *Advanced Drug Delivery Reviews*. 65(9):1215-1233 (2013).

[12] CO Onyeji. Cyclodextrin Complexes: Utility in Improving Drug Bioavailability and Other Applications. *Bioequivalence & Bioavailability International Journal*. 2(2): 130 (2018).